Published as: Rodgers, M., Kielty, A., **Healy, M.G**. 2014. Performance of granitic, shale, and limestone forest road aggregates subjected to repeated loading. ASCE Journal of Transportation Engineering 140(4): 47-54. **ISSN:** 0733-947X DOI: 10.1061/(ASCE)TE.1943-5436.0000654

The performance of granitic, shale and limestone forest road aggregates under repeated loading

M. Rodgers[1], A. Kielty[2], M.G. Healy[3]

ABSTRACT

This study compared the performance of three aggregate layerings, commonly used in the construction of unbound forest roads in Ireland, when they were subjected to repeated loading in a new large-scale test rig. These layerings comprised (i) a layer of uncrushed, granitic, sandy gravel - a good quality road aggregate (ii) a layer of shale - a poor quality aggregate, and (iii) a layer of crushed limestone – an excellent quality aggregate with a wet mix macadam (WMM) grading – on top of a poor quality shale sub-base layer . The repeated load testing rig was designed and constructed to test different surface or completion layering thicknesses of the aggregates over a common formation or subgrade

[1] Managing Director, Rodgers Morgan Environmental Ltd., Barna Road, Galway, Republic of Ireland.
[2] Graduate student, Civil Engineering, National University of Ireland, Galway, Republic of Ireland.
[3] Lecturer, Civil Engineering, National University of Ireland, Galway, Republic of Ireland (corresponding author). Email: mark.healy@nuigalway.ie

material of silty sandy soil. This testing was achieved by surface loading the aggregates through a 200 mm-diameter rubber pad - attached to a hydraulic actuator on the test rig - for up to 150,000 load applications. The subgrade pressures and surface deflections were measured at applied stresses of 500 kPa, 750 kPa and 1000 kPa. The good quality granitic aggregate performed much better than the poor quality shale aggregate under the repeated loading and is suitable as a completion material for use in unbound forest roads. The shale aggregate can be used in unbound forest roads as a sub base material.

CE Database subject headings: Access roads; aggregates; load bearing capacity; load tests; loads; forests.

INTRODUCTION

The Irish forestry company, Coillte Teoranta, is the biggest constructor of unbound roads in Ireland and builds approximately 300 km of new and upgraded roads per year. Forest roads should ideally be constructed using high quality aggregates. These roads should be built as economically as possible, while achieving a standard of road that is structurally capable of doing its job. In many areas in Ireland these quality aggregates are not available locally. In some cases a decision has to be made between importing higher quality material at high prices, or using greater thicknesses of poorer local material in the road construction.

The pavement layers in unbound forest roads are normally defined as follows:

(1) the formation layer is the underlying prepared *in-situ* soil under the road, more commonly known as the subgrade.

(2) the completion layer is the top layer of the road. In forest road construction, the completion layer can be constructed from suitable local aggregates. If it's necessary to place a layer of imported aggregate on top of a layer of local aggregate, then the local aggregate layer is commonly known as the sub base.

Well graded aggregates of high strength and durability, and compacted at their optimum water content (OWC), can form a strong road pavement completion layer that reduces the transfer of excessive applied stresses from moving vehicular wheels to lower strength sub base and subgrade layers. Also, the sub base and subgrade layers must be of adequate thickness, compaction and strength to accommodate, at acceptable deformations, the stresses transferred through the completion layer.

Kennedy (1985) and Dawson et al. (1993) stated that suitable materials for granular layers in a road pavement should have a high stiffness to give good load spreading properties, and high shear strength to reduce rutting under construction traffic. They should also have a high permeability to allow surface water to drain freely and quickly, have non-plastic fines to maintain strength under wet conditions and not be susceptible to frost damage (Kennedy 1985). Unbound roads with a high proportion of unsuitable fine-grained completion material may be subject to surface disintegration due to its low shear strength (Simonsen and Isacsson 1999; Lekarp et al. 2000). As the contact pressure from a tire is mainly supported by the completion layer, the load from the tire can increase the pore water

pressure in the road material when drainage is restricted. This pore water pressure increase can make unsuitable completion material unstable and may result in permanent deformation of the road surface (Simonsen and Isacsson 1999).

Indentations, called ruts, can develop at the surface of the completion layer over time. The rut depth, s (mm), may be calculated for geosynthetic, reinforced pavements from Giroud and Han (2004a):

$$s = \frac{\frac{P}{\pi r^2} f_s}{\left[\frac{h + 0.204h(R_E - 1)}{0.868r + r(0.661 - 1.006J^2)\left(\frac{r}{h}\right)^{1.5} \log N} + 1\right]^2 \left[\left[1 - 0.9\exp\left[-\left(\frac{r}{h}\right)^2\right]\right] N_C c_u\right]} \quad [1]$$

where J is the aperture stability modulus of the geogrid (m N/^{o}); r, the radius of the equivalent tire contact area (m); h, the depth of the completion layer (m); N, the number of loading cycles; P, the wheel load (kN), N_c, the bearing capacity factor; f_s, the maximum allowable rut depth (75mm); and c_u, the undrained cohesion of the formation layer (kPa). The limited modulus ratio, R_E, can be calculated from Giroud and Han (2004a):

$$R_E = \min\left(\frac{E_{cl}}{E_{fl}}, 5.0\right) = \min\left(\frac{3.48CBR_{cl}^{0.3}}{CBR_{fl}}, 5.0\right) \quad [2]$$

where E_{cl} and E_{fl} are the completion layer and formation layer resilient moduli, respectively (MPa), and CBR_{cl} and CBR_{fl} are the California Bearing Ratios (%) of the

completion layer and formation layer aggregates, respectively. The design method of Giroud and Han (2004a) is unique insofar as it is theoretically based and experimentally calibrated, and the inter-relationships between various parameters (stress distribution, traffic volume, rut depth, etc.) are contained within a single equation, whereas more than one equation was needed with earlier methods (Giroud and Noiray, 1981; Giroud et al. 1985).

The study objectives were:

1. To design and build a repeated load testing machine that establishes the efficacy of using locally available aggregates in unbound forest road construction.
2. To collect, classify and perform repeated load tests on three aggregate materials that are currently used, singly or in combination, by Coillte Teoranta in Ireland for forest road construction. These materials were a good quality granite aggregate, a poor quality shale aggregate and a crushed limestone with a wet mix macadam grading (WMM).
3. To model the performance of the unbound aggregates using the finite element program, SIGMA/W, and Equations 1 and 2.

MATERIALS AND METHODS

Aggregate testing

The formation material consisted of a silty, sandy soil with small amounts of clay from Castledaly, County Galway. This soil was cohesive and was representative of subgrade soils found in Ireland. The three completion materials examined were a good quality granite aggregate from the Wicklow/Wexford region, a poor quality shale aggregate from the Leitrim region and a crushed limestone from a Galway quarry. The Wicklow/Wexford aggregate was an uncrushed, granitic, sandy gravel. It was chosen as the main sample for testing because its grading curve was almost entirely within the grading envelope for a wet mix macadam (WWM, Clause 810). The second aggregate was a shale and was extracted from a pit situated in the Arigna mountains near the village of Drumkeeran, Co. Leitrim. This aggregate is a mud shale, is soft and fissile, and disintegrates rapidly under loading and weathering. The crushed limestone, which is often used as completion material on top of poor local aggregates by Coillte Teoranta, was obtained from a quarry outside Galway City and graded to the specification of a WWM.

Classification tests, including tests for natural water content, Atterberg limits, specific gravity and particle size distribution, were carried out on both the formation and the completion materials in accordance with BS 1377 (1990).

The completion materials were also tested for durability - a measure of an aggregate's resistance to environmental influences like wetting, thermal expansion/contraction and freeze/thaw effects. Durability was tested using the magnesium sulphate soundness value (MSSV) test and the water absorption value (WAV) test. In bound roads, an MSSV > 75% is required for all road base and sub base aggregates, and a WAV < 2% is required for most road aggregates (BSI 812, 1990). The strength of the completion layer aggregates

130 was also tested using the Aggregate Crushing Value (ACV) (BS 812 1990), the 10% Fines
131 Value (TFV) (BS 812 1990), the Aggregate Impact Value (AIV) (BS 812 1990), the
132 Aggregate Abrasion Value (AAV) (BS 812, 1990), and the California Bearing Ratio
133 (CBR) (BS 1377 1990). In the field, the CBR of the completion material is dependent on
134 the CBR of the formation (Giroud and Han 2004b). The cohesive strength of the formation
135 material, c_u, was determined from the direct shear test (BS 1377 1990).
136
137 Placement of materials and instrumentation
138
139 The completion layer aggregates were compacted in a bin, on top of the 1000 mm-thick
140 formation material, and tested at different thicknesses. The edges of the bin were sealed
141 with silicone mastic and the bin was lined with a double layer of polythene. This was to
142 ensure equilibrium of soil-water in the formation layer and to reduce friction along the bin
143 sides. The formation material was compacted in the bin close to its maximum dry density
144 as determined by the Proctor test (BS 1377 1990). Approximately 2,700 kg of soil was
145 dried below the OWC, using an industrial gas heater, and placed in plastic bags, after
146 removing particle sizes greater than 20 mm. The mass and water content of each bag of
147 soil was calculated and recorded. The appropriate mass of water was added and mixed to
148 each sample to increase the water content to its optimum value. The bags were then sealed
149 to allow the soil-water to equilibrate. The soil was compacted in 50 mm layers in the bin to
150 a height of 1000 mm, using a vibrating hammer with a 150 mm x 150 mm plate and an

applied force of approximately 400 N. Water contents were taken at each layer and an average water content was calculated. The dry density and water content of the soil was also monitored using a nuclear density probe, at different heights, as the soil was placed. The preparation of the formation layer took approximately 4 - 5 weeks.

The completion materials were compacted, in 50 mm layers, close to their maximum dry density as determined by the vibrating hammer test. All particles significantly greater than 50 mm were removed from the completion materials to aid compaction. This removal had no significant change on the particle size distribution of the granite, but made the particle size distribution of the shale finer. The dry density and water content of the compacted materials were monitored using a nuclear density probe.

The resilient and permanent deflections, and resilient pressures in the soil, which occurred on load application, were measured using displacement linear strain conversion transducers (lscts) (MPE Transducers Ltd., UK), and hydraulic pressure cells, all with excitation voltages of 10 volts d.c. and an output range of 0-200 millivolts d.c. (resilient behaviour is also referred to as recoverable or elastic behaviour). The lscts were calibrated using a micrometer block and a computer program (LabVIEW^{TM}, National Instruments Ltd., Austin, USA) before use. The spindle axis of each soil surface lsct, as well as of each of two standard dial gauges, were positioned along a vertical plane that coincided with the central vertical axis of the loading pad, as shown in Figure 1. The maximum spindle travel distances of the lscts used in this study varied between 15 mm and 25 mm, the larger being positioned nearer the central vertical axis of the pad.

As the formation soil was being placed and compacted in the soil bin of the test rig, four 100 mm diameter x 6.5 mm deep pressure cells were positioned horizontally in the formation material (Figure 1) at heights of 300 mm (D), 500 mm (C), 700 mm (B) and 900 mm (A) above the soil base, with their centers coincident with the central vertical axis of the loading pad. Two 0-10 bar cells were placed towards the top of the bin at positions C and D, one 0-5 bar cell at position B and one 0-2 bar cell at position A.. The pressure cells were calibrated in a water-filled triaxial cell at a range of appropriate cell pressures. When placing the pressure cells, the soil was compacted to a height of 25 mm above the desired height of the cell. A 50 mm-deep recess for the cell and cables was then dug out of the compacted soil. Layers of coarse-to-fine soil were placed under and over the cells, with the fines closest to the face of the cells. The next 50 mm layer of soil was added and compacted. This method of placement protected the pressure cells from possible damage due to compaction, as there was at least 75 mm of soil between the pressure cell and the vibrating hammer. Rubber tubing was placed along the pressure cell cables for extra protection.

Loading rig construction

A repeated-load testing machine was designed and constructed to apply pressures, similar to that of a truck tire, to the aggregate materials (Figure 1). The load frame was designed to withstand several hundred thousand cycles of loading up to 40 kN with minimal

196 deflections. It comprised two simply supported steel frames of universal beams (Steel
197 Grade 43) constructed in parallel on common steel base-plates. 305 x 165 UB 40 sections
198 were used for both the beams and columns. Two No. 700 x 700 mm holes were broken out
199 of the existing concrete floor and eight No. M20 Gr. 8.8 x 180 bolts were sunk to a depth
200 of 140 mm in a 200 mm depth of C40 concrete (28 day strength = 40 N mm^{-2}) to provide a
201 suitable reaction for the base-plates of the frame. Flat strips of metal were welded to the
202 ends of the bolts to ensure complete grip in the concrete.
203
204 The design of the loading pad was similar to that used by Davitt (1982). The pad
205 comprised a 200 mm diameter x 45 mm thick rubber disc (Dunlop, England) and was
206 identical to that used in truck tires. The rubber was bonded to a robust steel frame, which
207 was bolted to a universal joint which, in turn, was screwed onto the end of the actuator
208 piston. The purpose of the universal joint was to ensure that the surface of the pad
209 remained parallel to the surface of the soil should any differential deformation occur
210 during testing. In this study, vertical pressures were applied to the unbound surface layer,
211 and resulted in a combination of vertical, horizontal and shear stresses in the completion
212 and formation layer materials. Similar loading techniques have been used in other studies
213 (Moghaddas Tafreshi and Khalaj, 2007).
214
215 The whole system was controlled and monitored by a programmable servo-amplifier that
216 was mounted within an electrical enclosure. The programmable servo-controller (PSC) was
217 programmed to drive the actuator to the desired loading cycle. The loading cycle had a 3-
218 second duration (frequency = 0.33 Hz.), and comprised 1 second of loading and 2 seconds
219 of recovery. Different levels of loading were applied in a cyclic manner to the aggregate

material. Each level of loading was applied for a maximum of 50,000 cycles. The average contact area of a truck tire on a road is 175 mm x 225 mm (0.0394 m^2). A load of 29.43 kN over this area yields an applied pressure of 746 kPa.

The loading procedure adopted was as follows:

50×10^3 cycles at an applied pressure of 500 kPa (lightly-loaded axle)

50×10^3 cycles at an applied pressure of 750 kPa (normally-loaded axle)

50×10^3 cycles at an applied pressure of 1000 kPa (heavily-loaded axle).

The two lower loadings provided a level of conditioning in the completion material, which can occur on a forest access road during drainage and tree planting activities in peatland, and during about 20 years of limited site service traffic prior to harvesting and extraction of the tree trunks, which would subject the road to the heaviest loading. Unpaved roads are typically designed for 100,000 axle passes (Giroud and Han 2004a), so this test examined the performance of the aggregates in an extreme loading scenario.

The physical responses measured during the repeated load testing on the completion materials were:

(1) permanent surface deformation versus number of loading cycles using the lscts and dial gauges

(2) resilient surface deflections versus number of loading cycles

(3) resilient pressures in the pressure cells, located in the formation soil directly under the loading pad .

The completion material and the top 50 mm layer of the formation material were removed after each test. The top 50 mm layer was replaced with soil compacted at its OWC. A previous study on a similar completion material, 150 mm deep, which was subjected to 50 $x10^3$ cycles at 500 kPa, followed by 50 $x10^3$ cycles at 750 kPa and 50 $x10^3$cycles at 1000 kPa, resulted in little deformation in the formation material (about 2 mm) at the higher maximum resilient pressures (Rodgers et al., 2009). As the formation material was compacted in 50 mm layers, it was considered adequate to remove only the top 50 mm layer.

Six full-scale tests were performed on the different materials and are listed in Table 1. Surface deformations of the completion layer and resilient pressures in the formation layer were measured during cyclic loading for the following road structure arrangements and conditions: (i) 250 mm-deep (Test 1) and 150 mm-deep (Test 2) layers of granite, and 250 mm-deep (Test 3) layer of shale completion materials; (ii) capping of a 250 mm-deep shale layer with 200 mm-deep (Test 4) layer of crushed limestone graded to the specification of a WMM (a well-graded crushed rock); (iii) the effect of water addition to the surface of the limestone (Test 5), and (iv) the 1000 mm-deep formation soil on its own (Test 6). In Tests 1-5 the completion materials were tested on top of the 1000 mm deep formation soil. For Test 4, 200 mm of a crushed limestone was compacted at a water content of 3.3% onto a 250 mm layer of the shale to determine if the shale would perform satisfactorily as a sub base material. After completion of this 150 x 10^3 cycle test, 10 mm of water was sprayed

onto the surface of the limestone and allowed to soak for one hour. This test (Test 5) was then started at an applied pressure of 500 kPa for a duration of 4 x 10^3 loading cycles and a comparison was made between the physical responses of this unbound layering in the dry state and in the wet state. In Test 6, the formation soil was tested under a repeated loading of 150 kPa without a completion material to determine its performance, and to provide resilient data for finite element program calibration to estimate E values for the formation soil. Approximately 3 - 4 weeks were required for the preparation, loading and analysis of Tests 1-4, 6.

Identification of model parameters

The validity of Eqn. 1 for the prediction of the rut depth, s, was investigated by comparing the measured versus the predicted values of s. As the aggregates were un-reinforced and unpaved, J = 0 and N_c=3.14. The radius of the tire contact area, r, was 0.1 m. As Eqn. 1 is only valid for CBR_{fl} ratios less than or equal to 5 (Giroud and Han 2004a), the E-values of the formation and completion layers were used to calculate R_E. In order to estimate the E values of the formation and completion materials for Eqn. 1, a series of elastic-plastic simulations with estimated E values were conducted using SIGMA/W (SIGMA/W, GEO-SLOPE International Ltd., Alberta, Canada), until the resilient pressures and deflections from these simulations were close to those recorded in the repeated loading experiments carried out in the test rig. The formation and completion material cohesion, c, and soil

285 friction angle, Φ, - some of the parameters required for SIGMA/W to model residual
286 responses - were determined from shear box tests. The Poisson's ratio, υ, for the formation
287 and completion material was after Evdorides and Snaith (1996).
288
289 SIGMA/W contains three separate programs, Define, Solve and Contour. The Define
290 program involves the plotting of the system geometry. Numeric parameters are defined by
291 manually inputting the values. The Solve program is used to compute the deformations and
292 stress changes. The Contour program graphs the computed parameters. SIGMA/W
293 comprises eight elastic and plastic constitutive soil models, all of which may be applied to
294 two-dimensional plane strain and axisymmetric problems. From the graphs of permanent
295 deformation versus number of cycles, all the materials tested showed signs of plastic
296 behavior due to their continual increase in permanent deformation with increasing number
297 of loading cycles. The elastic-plastic model was therefore used to model the experimental
298 results.
299
300 RESULTS AND DISCUSSION
301
302 Placement of materials
303
304 The granite aggregate was compacted at an average water content of 6.6 % (OWC, 8.3%)
305 with an average dry density of 2.1 Mg m^{-3}; the shale was compacted at an average water
306 content of 9.1% (OWC, 10.3%) with an average dry density of 1.5 Mg m^{-3} (Table 1).
307
308 Soil classification tests

309

310 The results from the soil classification tests are shown in Table 2 and the particle size
311 distributions are in Figure 2. The formation was a well-graded formation soil, achieving
312 high levels of strength, with a CBR of 15%, when compacted at its OWC. This soil was
313 sensitive to water - an increase of 3% in water content resulted in a reduction in CBR to
314 2%.

315

316 The shale aggregate was a mud shale; poorly graded, flaky and lacking in fines, making it
317 difficult to compact. The aggregate was low in strength and durability. The results of the
318 ACV and the AIV tests for the shale, tested in its dry state, indicated that it could just meet
319 most specifications for these tests. However, the CBR of the proposed shale completion
320 aggregate was only 25.2% at its OWC and the ratio of its CBR ratio to that of the
321 formation material (15% at OWC) was less than 2, indicating that a completion shale layer
322 might not provide adequate strength in unbound road construction (Hammitt, 1970). The
323 granite was a well-graded, sandy gravel, achieving high degrees of compaction. The
324 aggregate was high in strength and durability and the CBR ratio of the granite to the
325 formation material was approximately 7. The limestone aggregate had good strength and
326 durability, was relatively well-graded and the CBR ratio of the limestone aggregate to the
327 formation material was approximately 10.

328

329 Resilient pressures

In Test 1 (250 mm of granite), the pressure in Cell D (100 mm from the surface of the formation material), for an applied pressure of 1000 kPa, was approximately 98 kPa (Figure 3). In Test 2 (150 mm of granite), a reduction in the completion layer thickness from 250 mm to 150 mm resulted in an increase in the Cell D pressures. Test 3 (250 mm of shale) was stopped after $10x10^3$ cycles, at an applied pressure of 500 kPa, due to excessive deformations of the material. The pressures in Cell D in Test 3 increased from an initial value of 64 kPa to 104 kPa, suggesting a consistent weakening of the shale under loading. It can be concluded that the shale is a poor road making material; it failed dramatically under the low pressure of 500 kPa. This poor performance may be due, in part, to the low CBR ratio between the completion and formation materials (Giroud and Han 2004b). In Test 4 (200 mm of limestone aggregate on 250 mm of shale), the pressures in Cell D, at an applied pressure of 500 kPa, increased only from 31 kPa to 38 kPa in approximately 30 x 10^3 cycles of loading in comparison with the increase from 64 kPa to 104 kPa for the shale completion material at the same applied pressure in Test 3. After the $150x10^3$ cycle test on the limestone over shale sub base was completed, the material was wetted, and the test was restarted at the applied pressure of 500 kPa for a duration of $4x10^3$ cycles (Test 5), during which the pressures in Cell D increased from 50 kPa to 57 kPa (Figure 3) - an increase of about 55% due to the addition of the water.

Resilient deflections

The maximum resilient deflection at the centre of the loading pad in Test 1 (250 mm of granite) was approximately 1.2 mm for an applied pressure of 1000 kPa (Figure 4). In Test

354 2, a reduction from 250 mm to 150 mm in the granite thickness resulted in a maximum
355 resilient deflection of 1.6 mm for an applied pressure of 1000 kPa, a 33% increase on the
356 maximum deflection measured at the same pressure in Test 1. In Test 5 the addition of
357 water to the limestone aggregate layer had a significant negative effect on its performance
358 under loading. The maximum resilient deflection measured, at an applied pressure of 500
359 kPa, ranged from 0.72 mm - 0.8 mm in the dry state to 1.15 mm - 1.2 mm in the wet state -
360 an average increase of 55%. Zakaria and Lees (1996) also found that the deflections of
361 densely graded brick and quartz aggregates, when wetted, increased considerably under
362 pressures of 210 kPa at less than 2000 cycles of loading.
363
364 Permanent deformations
365
366 In Test 1, the overall permanent deformation in the 250 mm-thick granite completion layer,
367 directly under the loading pad, was 4.5 mm (Figure 5) after 150 x 10^3 cycles. This was not
368 very much different from the surface deformation for the 150 mm granite completion layer
369 in Test 2. The addition of the limestone layer on top of the shale in Test 4 improved on the
370 performance of the shale alone in Test 3 but the limestone/shale performance was still
371 poorer than the performances of the two granitic completion layers. The combined
372 limestone/shale layering in Test 4 produced significantly lower resilient stresses than in
373 Test 3 and prevented any deformation occurring in the formation material. However, the

374 permanent deformations were much greater for the combined material test (Test 4) than for
375 the granite completion layers in Tests 1 and 2.
376
377 Prediction of rut depths under repeated loadings
378
379 As all the materials tested showed a continual increase in permanent deformation with
380 increasing number of loading cycles (Figure 5), the elastic-plastic SIGMA/W model was
381 used in modelling the experimental results. The effectiveness of Eqn. 1 in predicting rut
382 depths is dependent on: (i) the measured undrained cohesion of the formation soil and (ii)
383 the E values of the formation and completion materials, estimated from SIGMA/W.
384 Estimates of the E-values were made through calibrating resilient pressure and deflection
385 values from the finite element model, SIGMA/W, with results measured in the rig
386 experiments, and these E estimates are given in Table 3. The E values for the formation
387 soil were estimated firstly from the resilient pressures and deflections measured in Test 6.
388 These formation E estimates were then used to estimate the granite aggregate E values
389 from the resilient results in Tests 1 and 2; Table 4 shows the excellent calibration achieved
390 for the 250 mm thick granite aggregate layer - also excellent for the 150 mm thick granitic
391 layer. The shale aggregate E value was obtained similarly from the resilient results in Test
392 3, but the calibration was only moderate for the shale aggregate. The limestone aggregate E
393 value was then estimated from calibrating the Test 4 resilient results using the previously
394 calibrated formation and shale E estimates; this Test 4 calibration was good for the
395 limestone/shale aggregates.
396

397 The estimated E values of the granite - for similar stresses and densities used in the present
398 study - were close to those given by (i) Hopkins et al. (2007) in their Figure 40, and (ii)
399 Boudali and Robert (1997) from the equation for resilient modulus, $M_R = k_1 . \theta^{k}_{2}$, where,
400 for a granite aggregate, k_1 has a value of 8139 kPa, k_2 a value of 0.6, and θ is the sum of
401 the principal stresses. The estimated E values of the limestone aggregate appear low in
402 comparison with the granite values, particularly at the higher applied pressures of 750 and
403 1000 kPa; this could have resulted from the availability of only an estimated E shale
404 aggregate value at the low pressure of 500 kPa in Test 3.
405
406 The estimated E values from SIGMA/W were used to predict the rut depths (permanent
407 deformations) in the granite aggregates at three cycles – 50,000, 100,000 and 150,000 - for
408 Tests 1 and 2 using Eqn. 1 (Table 5). When the E values of 29 MPa for the top 50 mm of
409 the formation layer and 37 MPa for the formation soil below the top 50 mm layer were
410 used in SIGMA/W, the simulated results of the permanent deformations in the two granite
411 aggregate completion layers were within 2 mm of those measured in the loading rig.
412
413 The calculated and modeled rutting depths were of the same order as other studies. Zakaria
414 and Lees (1996) measured rut depths of between 4 and 9 mm in brick and quartz
415 aggregates, which were subjected to a tire contact pressure of up to 210 kPa in laboratory
416 experiments. In the same study, the rut depth increased by between 30 and 80% when the
417 material was saturated (the water content was not specified in the study). Other factors

418 such as tire inflation and wheel load may also impact on rut depth, as Douglas (1997)
419 found that significantly shallower ruts formed in a Gault clay aggregate, subjected to
420 tracking wheel loads at up to 10,000 passes, when the tire inflation pressure was reduced
421 from 690 kPa to 345 kPa.
422
423 CONCLUSIONS
424
425 The main observations from the testing were:
426
427 1. The formation material was a well graded soil capable of high strength when
428 compacted at the OWC; however, its strength reduced significantly when the water content
429 increased by 2 – 3 % above the optimum.
430 2. Granite aggregate, with a thickness of just 150 mm, is a good completion material
431 capable of supporting applied pressures of 1000 kPa for 50,000 cycles with resulting
432 permanent deformations of less than 5 mm.
433 3. Shale at a depth of 250 mm is a poor quality completion aggregate, but can be
434 made serviceable with a 200 mm top layer of high quality limestone aggregate.
435 4. The use of Eqn. 1 to estimate the rut depth for un-reinforced, unpaved granite
436 aggregate gave permanent deformations within 2 mm of the experimental measurements.
437 5. The resilient performance of granitic aggregate on top of a silty sandy formation
438 soil can be modeled using the finite element program SIGMA/W.
439
440 ACKNOWLEDGEMENTS
441

442 This project was part funded by the Council for Forest Research and Development
443 (COFORD) under the operational Programme for Agriculture, Road Development and
444 Forestry, supported by EU structural funds. Financial support was also obtained from
445 Coillte Teoranta. The authors would like to express their appreciation to the late Dr. John
446 Mulqueen, NUI, Galway.
447
448 REFERENCES
449 Boudali, M., and Robert, C. (1997). "Détermination en laboratoire du module réversible
450 des matériaux de fondations. Transport Québec. In: Receuil des communications 32
451 Congrès de l'AQTR, Tome 2, pp. 107-128.
452
453 BS 1377 (1990). *Method of test for soils for civil engineering purposes*. London: British
454 Standard Institution, London.
455
456 BS 812 (1975, 1989, 1990). *Methods for sampling and testing mineral aggregates, sands*
457 *and fillers.* London: British Standard Institution, London.
458
459 Davitt, J. (1982). Repeated load tests on simulated gravel pavements from three sources in
460 Ireland. Dissertation, University of Dublin.
461

462 Dawson, A.R., Paute, J.L., and Thom, N.H. (1993). “Mechanical characteristics of
463 unbound materials as a function of condition”. In: Proceedings of the European
464 Symposium on Flexible Pavements, Euroflex. 199, Rotterdam, pp 35-44.
465
466 Douglas, R.A. (1997). “Heavy load, low tire pressure rutting of unbound granular
467 pavements”. *J. Trans. Eng.,* 123, 357 – 363.
468
469 Evdorides, H.T., and Snaith, M.S. (1996). “A knowledge-based analysis process for road
470 pavement condition assessment”. *Proceed. ICE – Transport*, 117, 202 – 210.
471
472 Giroud, J.P., and Noiray, L. (1981). “Geotextile-reinforced unpaved road design.” *J.*
473 *Geotech. Eng.*, 107, 787 – 797.
474
475 Giroud, J.P., Ah-Line, C., and Bonaparte, R. (1985). “Design of unpaved roads and
476 trafficked areas with geogrids.” *Polymer grid reinforcement,* Thomas Telford Limited,
477 London, 116 – 127.
478
479 Giroud, J.P., and Han, J. (2004a). “Design method for geogrid-reinforced unpaved roads.
480 II. Calibration and applications”. *J. Geotech. and Geoenv. Eng*., 130, 787 – 97.
481
482 Giroud, J.P., and Han, J. (2004b). “Design method for geogrid-reinforced unpaved roads. I.
483 Development of design method”. *J. Geotech. and Geoenv. Eng.,* 130, 775-85.
484

485 Hopkins, T.C., Beckham, T.L., Sun, C. (2007). "Resilient modulus of compacted crushed
486 stone aggregate bases." Research Report KTC-05-27/SPR-229-01-1F.
487 http://uknowledge.uky.edu/cgi/viewcontent.cgi?article=1179&context=ktc_researchreports
488 (accessed 20 November 2013)
489
490 Hammitt, G.M. (1970). Thickness requirement for unsurfaced roads and airfields, bare
491 base support, project 3782-65. Technical report S-70-5, Vicksburg, Miss., U.S. Army
492 Engineer Waterways Experiment Station.
493
494 Kennedy, C.K. (1985). "In-situ testing of unbound aggregates". In: Proceedings of the
495 Symposium on unbound aggregates in Roads, Nottingham, University of Nottingham, pp
496 63-68.
497
498 Lekarp, F., Isacsson, U., and Dawson, A. (2000). "State of the art: I: Resilient response of
499 unbound aggregates". *J. Trans. Eng.,* 126, 66 – 75.
500
501 Moghaddas Tafreshi, S.N., and Khalaj, O. (2007). "Laboratory tests of small-scale HDPE
502 pipes buried in reinforced sand under repeated load". *Geotext. and Geomem.*, 26, 145 –
503 163.
504

Rodgers, M., Hayes, G., and Healy, M.G. (2009). “Cyclic loading tests on sandstone and limestone shale aggregates used in unbound forest roads”. *Const. Build. Mat*., 23, 2421-2427.

Simonsen E., and Isacsson, U. (1999). “Thaw weakening of pavement structures in cold regions”. *Cold Reg. Sci. Tech*., 29, 135 – 151.

CAPTIONS FOR FIGURES

Figure 1 The laboratory loading apparatus.

Figure 2 Particle size distributions for the materials.

Figure 3 Resilient pressures in Cell D, measured 900 mm above the base of the formation layer, versus number of cycles.

Figure 4 Maximum resilient deflections measured at the surface of the completion layer versus number of cycles.

Figure 5 Maximum permanent deformations measured at the surface of the completion layer versus number of cycles.

Table 1. List of full-scale tests.

Test number	Material	Thickness [a]	Optimum water content	Initial water content	Final dry density
		m	%	%	Mg m^{-3}
1	Granite	0.25	8.3	6.6	2.1
2	Granite	0.15	8.3	6.3	2.0
3	Shale	0.25	10.3	9.1	1.5
4	Limestone on top of shale [b]	0.20+0.25		3.3	
5	Limestone on top of shale with water addition	0.20+0.25		3.3	
6	Formation layer	1.00	13.5	13.6	1.5

[a] Thickness refers to the completion layer. The formation material had a thickness of 1000 mm for all tests.

[b] 200 mm of a crushed limestone, graded to the specification of a wet mix macadam, was compacted, at a water content of 3.3%, onto a 250 mm layer of the shale at a water content of 9.1%.

566 Table 2. Summary of BS laboratory results.

Laboratory tests	Limits	Formation	Completion		
			Granite	Shale	Limestone
Natural water content (%)		21.5			
Liquid limit		32.3	43.8	52.4	18.3
Plastic limit (%)		22.6	NP	33.9	NP
Plasticity index (%)	0-6	9.7	0	18.5	0
Specific gravity (Gs)		2.6	2.7	2.5	2.7
Max. dry density (Mg m^{-3})		1.8	2.2	1.6	2.3
Optimum water content (%)		13.5	8.3	10.3	6.1
California bearing ratio (%) [a]	2/30	15.0	115.0	25.2	156.0
Flakiness index (%)	<35.0		26.4	78.0	19.6
MSSV (%)	>75.0		92.9	10.1	93.8
Water absorption value (%)	<2.0		2.9	6.2	0.3
Aggregate crushing value (%)	<35.0		18.5	34.2	21.3
Dry aggregate impact value (%)	<35.0		17.5	31.0	15.2
Wet aggregate impact value (%)			18.6	37.0	
Aggregate abrasion value (%)	<10.0		2	39.2	11.0
Effective size, d_{10}, (mm)		$3.9x10^{-3}$	$1.7x10^{-1}$	5.5	0.7
Uniformity coefficient, C_u		44.9	73.5	8.2	15.0
Coefficient of curvature, C_c		0.7	1.2	1.6	3.4

567 [a] The minimum allowable in situ CBR for a subgrade soil is 2%. Type A sub base material should have a
568 CBR of 30%.
569
570
571
572
573
574
575
576

577 Table 3. Estimation of resilient moduli [a]

Material	Thickness	Applied pressure (kPa)		
		500	750	1000
	m	Calculated resilient moduli, E (MPa)		
Formation	0 – 0.05	29	29	29
	0.05 – 1	37	37	37
Granite	0.25	295	450	550
Granite	0.15	320	460	750
Shale	0.25	60		
Limestone on top of shale [b]	0.20+0.25	225	225	225

578 [a] The resilient moduli for the soils were estimated by calibrating the SIGMA/W finite
579 element model of the soils and loadings to provide resilient deflections under the centre of
580 the loading pad that were equal to the experimental results.
581 [b] 0.2 m of a crushed limestone, graded to the specification of a wet mix macadam, was
582 compacted, at a water content of 3.3%, onto a 0.25 m layer of the shale with an assumed
583 constant resilient modulus of 60 MPa for the three applied pressures
584
585
586
587
588
589
590
591
592

Table 4. Experimental and modelled values for resilient deflection at the surface layer of the completion material and pressure at depths of 0.1, 0.3, 0.5 and 0.7 m from the surface of the formation layer.

Soil physical responses	Test no.[a]	Applied pressure (kPa)					
		500		750		1000	
		Measured	Modelled	Measured	Modelled	Measured	Modelled
Resilient deflection (mm)	1	0.70	0.70	0.92	0.92	1.16	1.16
Pressure at 0.7m (kPa)	(250 mm	10.5	9.0	15.8	14.0	21.6	19.0
Pressure at 0.5m (kPa)	granite)	12.0	13.0	18.6	21.5	25.0	27.0
Pressure at 0.3m (kPa)		26.0	24.0	40.0	36.0	54.6	47.5
Pressure at 0.1m (kPa)		51.0	51.0	73.5	71.0	97.7	92.0
Modulus of elasticity (MPa)		295		450		550	
Resilient deflection (mm)	2	0.96	0.97	1.33	1.34	1.59	1.60
Pressure at 0.7m (kPa)	(150 mm	13.3	11.0	21.5	17.0	28.3	22.0
Pressure at 0.5m (kPa)	granite)	17.4	16.3	26.0	25.5	33.8	33.0
Pressure at 0.3m (kPa)		39.1	33.0	58.8	50.0	74.4	64.0
Pressure at 0.1m (kPa)		95.9	84.0	124.7	120.0	148.2	146.0
Modulus of elasticity (MPa)		320		460		750	
Resilient deflection (mm)	3	1.73	1.76				
Pressure at 0.7m (kPa)	(250 mm	15.1	10.0				
Pressure at 0.5m (kPa)	shale)	17.2	15.0				
Pressure at 0.3m (kPa)		44.6	30.0				
Pressure at 0.1m (kPa)		104.0	72.0				
Modulus of elasticity (MPa)		60					
Resilient deflection (mm)	4	0.76	0.76	1.2	1.18	1.6	1.6
Pressure at 0.7m (kPa)	(200 mm	9.07	5.7	11.9	9.8	15.5	13.8
Pressure at 0.5m (kPa)	limestone /	9.32	8.0	13.0	13.5	17.2	19.0
Pressure at 0.3m (kPa)	250 mm	17.3	13.5	26.4	22.0	32.5	31.0
Pressure at 0.1m (kPa)	shale)	38.0	24.0	50.3	39.0	57.3	54.0
Modulus of elasticity (MPa)		225		225		225	

[a] 1 - 0.25 m of granite; 2 – 0.15 m of granite; 3 – 0.25 m of shale; 4 – 0.2 m of limestone on 0.25 m shale

Table 5. Comparison of modelled (Eqn. 1) versus measured rut depths.

Material	Depth (m)	No of cycles					
		0 – 50,000 at 500 kPa		0 – 50,000 at 500 kPa 50,000 – 100,000 at 750 kPa		0 – 50,000 at 500 kPa 50,000 – 100,000 at 750 kPa 100,000 – 150,000 at 1000 kPa	
		Calculated (mm)	Measured (mm)	Calculated (mm)	Measured (mm)	Calculated (mm)	Measured (mm)
Formation	1						
Granite	0.25	1.1	2.6	2.6	3.6	4.4	4.5
Granite	0.15	2.1	4.1	4.6	5.0	7.4	6.0

Figure 1.

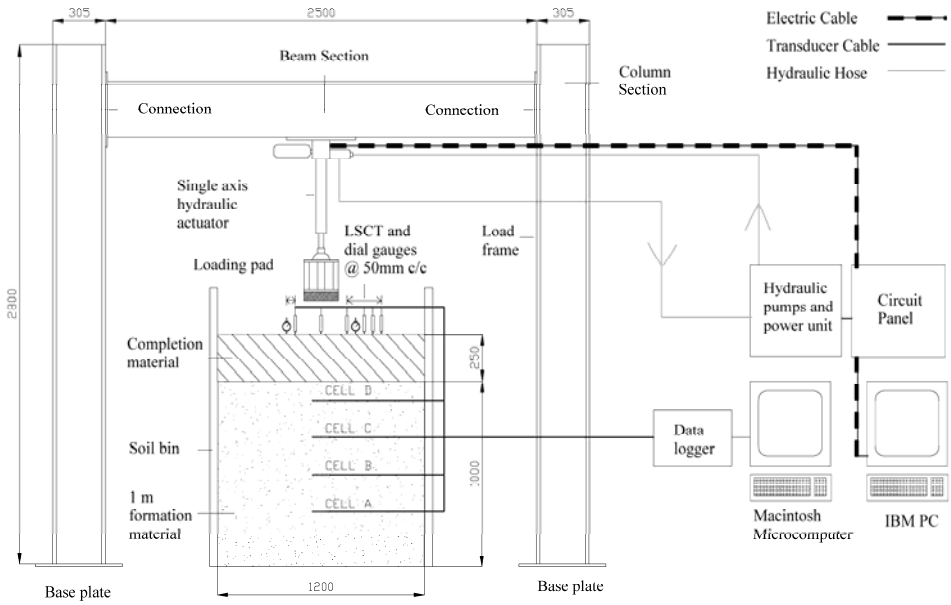
305
2500
305
Beam Section
Connection
Connection
Column Section
Electric Cable
Transducer Cable
Hydraulic Hose
Single axis hydraulic actuator
LSCT and dial gauges @ 50mm c/c
Load frame
Loading pad
2300
Completion material
250
CELL D
CELL C
CELL B
CELL A
Soil bin
1000
1 m formation material
1200
Base plate
Base plate
Hydraulic pumps and power unit
Circuit Panel
Data logger
Macintosh Microcomputer
IBM PC

Figure 2

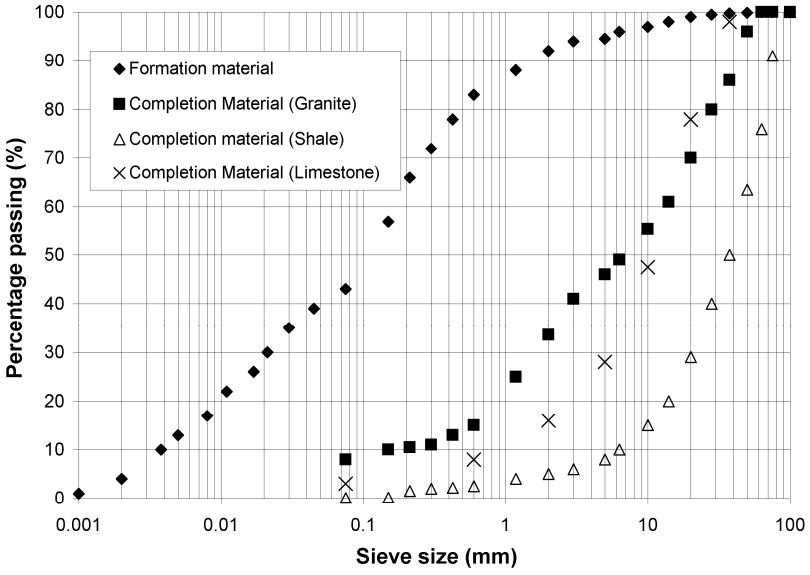
Formation material
Completion Material (Granite)
Completion material (Shale)
Completion Material (Limestone)
Percentage passing (%)
Sieve size (mm)
0
10
20
30
40
50
60
70
80
90
100
0.001
0.01
0.1
1
10
100

Figure 3

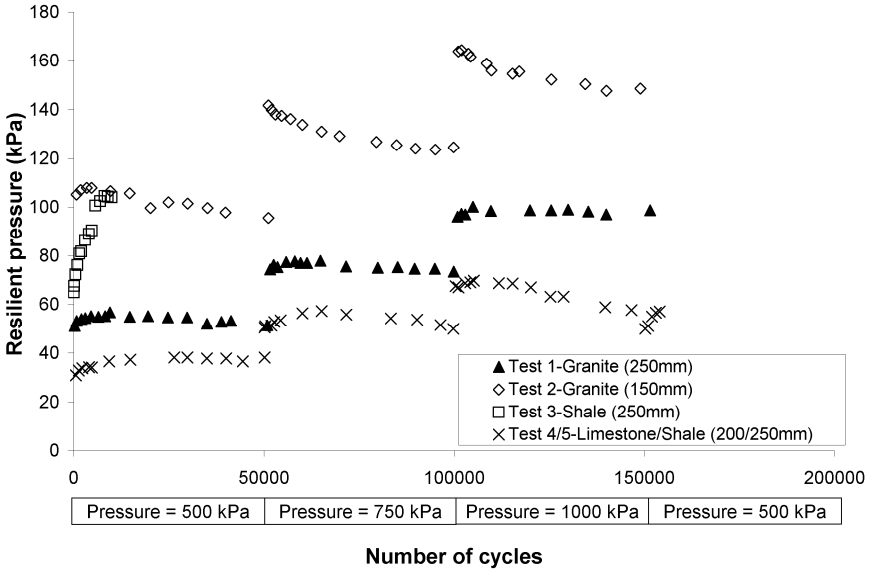
Resilient pressure (kPa)
180
160
140
120
100
80
60
40
20
0
0
50000
100000
150000
200000
Test 1-Granite (250mm)
Test 2-Granite (150mm)
Test 3-Shale (250mm)
Test 4/5-Limestone/Shale (200/250mm)
Pressure = 500 kPa
Pressure = 750 kPa
Pressure = 1000 kPa
Pressure = 500 kPa
Number of cycles

Figure 4

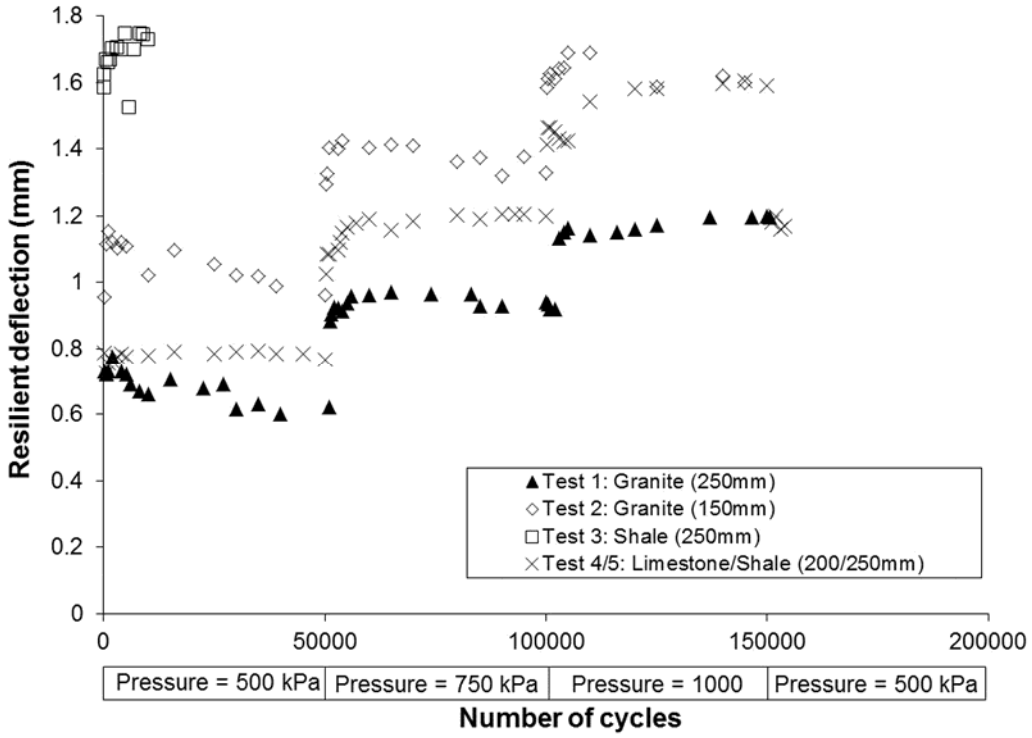
Resilient deflection (mm)
1.8
1.6
1.4
1.2
1
0.8
0.6
0.4
0.2
0
0
50000
100000
150000
200000
Test 1: Granite (250mm)
Test 2: Granite (150mm)
Test 3: Shale (250mm)
Test 4/5: Limestone/Shale (200/250mm)
Pressure = 500 kPa
Pressure = 750 kPa
Pressure = 1000
Pressure = 500 kPa
Number of cycles

Figure 5

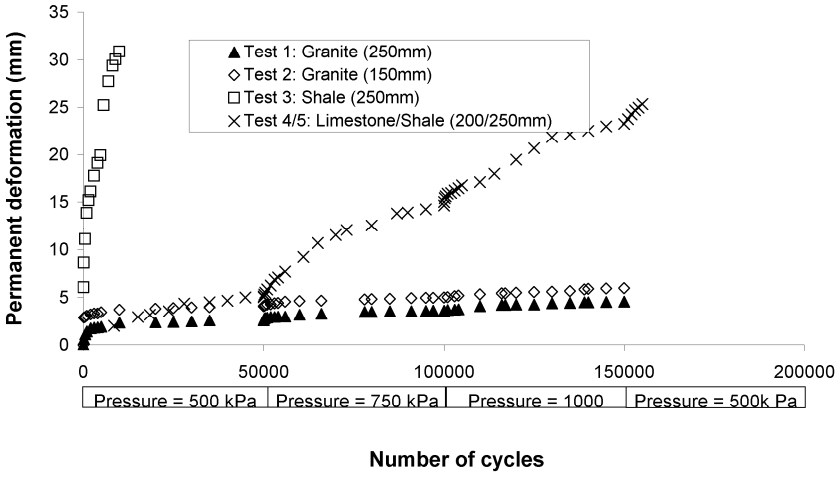
Permanent deformation (mm)
35
30
25
20
15
10
5
0
Test 1: Granite (250mm)
Test 2: Granite (150mm)
Test 3: Shale (250mm)
Test 4/5: Limestone/Shale (200/250mm)
0
50000
100000
150000
200000
Pressure = 500 kPa
Pressure = 750 kPa
Pressure = 1000
Pressure = 500k Pa
Number of cycles